Nonequilibrium Model for Sorption and Swelling of Bulk Glassy Polymer Films with Supercritical Carbon Dioxide

Vito Carla,[†,‡] Ke Wang,[†] Yazan Hussain,[†] Kirill Efimenko,[†] Jan Genzer,[†] Christine Grant,[†] Giulio C. Sarti,[‡] Ruben G. Carbonell,[†] and Ferruccio Doghieri*[,‡]

Department of Chemical and Biomolecular Engineering, North Carolina State University, Raleigh, North Carolina 27695, and Department of Chemical Engineering, University of Bologna, Bologna, Italy

Received March 31, 2005; Revised Manuscript Received July 27, 2005

ABSTRACT: A new procedure is introduced for the calculation of solubility isotherms of plasticizing agents in glassy polymer matrices with particular application to the case of absorption of supercritical gases in bulk glassy polymer films. The model presented is an extension of the nonequilibrium thermodynamics for glassy polymers (NET-GP) approach, modified to allow for the calculation of the effects of pressure, temperature, and gas concentration on the glass transition. Mass sorption and one-dimensional swelling behavior are analyzed for the carbon dioxide (CO_2)−poly(methyl methacrylate) (PMMA) system at high pressure. A quantitative comparison is presented between the model performance and experimental data measured using quartz crystal microbalance (QCM) and high-pressure ellipsometry (HPE).

1. Introduction

Carbon dioxide in its liquid and supercritical state is an attractive replacement for aqueous and organic solvents in industry primarily because of its tunable solvent properties, low cost, low toxicity, nonflammability, and its ease of recycle.[1−6] In addition, carbon dioxide is an excellent plasticizer for polymeric materials;[7−10] it is inert as a reaction solvent, and it has very low surface energy and viscosity, making it ideal for producing thin uniform coatings.[11−13] For these reasons, carbon dioxide has been used in several processes, such as polymerization reactions,[14] dry cleaning,[15] drug formulations,[16] foam production,[17] metal deposition onto substrates,[18] polymer surface modification,[19] and microelectronics fabrication,[20] and many applications, including polymeric membrane conditioning,[21] removal of residual solvents and contaminants from polymeric films,[22−24] solute impregnation,[25,26] and photoresist development.[27−29]

In most of the aforementioned industrial applications the key factor that influences the quality of the final product is the ability to predict sorption and consequent swelling behavior of the polymer matrix at different operating conditions. Indeed, a reliable thermodynamic model, capable of describing the swelling of glassy polymer systems starting from dry polymeric matrices up to fully plasticized materials, is an essential prerequisite of any good transport model aimed at predicting sorption, desorption, and dissolution kinetics in polymeric films. Because glassy polymers are nonequilibrium systems, the usual thermodynamic models for fluids and amorphous polymers, such as the Sanchez−Lacombe (SL) or the statistical associated fluid theory (SAFT) equation of state, are not directly applicable to these systems.

To fill this knowledge gap, a great deal of work has been done to obtain useful and reliable models for sorption and dilation in glassy polymers. Wissinger and Paulaitis were the first to apply successfully the nonequilibrium thermodynamics concept of an order parameter to an equilibrium lattice model.[30] Although their results were in good agreement with their experimental data, they used a constant order parameter with its value fixed at the glass transition conditions so that their model was unable to represent the significant solubility variations and hysteresis behavior associated with sorption−desorption cycles. Soon after their work, several models appeared in the literature based on the same approach but with a different choice of the order parameter.[31,32]

The Gibbs−DiMarzio criterion, which postulates a loss of configurational entropy at the glass transition temperature, was used by Condo et al. to develop a complete consistent theory for glassy systems through an extension of the classical Sanchez−Lacombe model.[33] Because this theory is a direct extension of the Sanchez−Lacombe lattice fluid theory, its predictive power is restricted to systems for which the Sanchez−Lacombe equation of state (EoS) is able to reproduce correctly the mixture behavior in the equilibrium region. However, there exist many real systems of importance for which this is not the case.

The main aim of this work is to introduce a new flexible model for mass uptake and swelling of glassy polymer films induced by the sorption of plasticizing agents, with special attention to the case of CO_2−polymer systems, over a wide range of pressures. This new model is an extension, to the case of plasticizing solutes, of the nonequilibrium thermodynamic model for solubility in glassy polymers (NET-GP), introduced by Doghieri and Sarti[34] and named NELF in its first version.[35−37]

The NET-GP model extends the free energy mapping for the equilibrium state, which can be obtained from any equations of state, to the nonequilibrium domain of the glassy region using a thermodynamically consistent procedure. The NET-GP approach requires that independent information be available for the mass

[†] North Carolina State University.
[‡] University of Bologna.
* To whom correspondence should be addressed. E-mail: Ferruccio.doghieri@mail.ing.unibo.it.

10.1021/ma0506684 CCC: $30.25 © 2005 American Chemical Society
Published on Web 10/27/2005

density of the polymer in the glassy state since this is used as an order parameter. Therefore, the first assumption of the NET-GP model is that the value of the order parameter, the out-of-equilibrium polymer density, determines the behavior of the system, regardless of the sample history through which this polymer density is achieved. Thus, the NET-GP approach cannot be used as a pure predictive tool because a value of the out-of-equilibrium polymer mass density must be available. It should also be stressed that the latter, being a nonequilibrium property, depends, in the most general case, on the thermal, mechanical, and sorption history of the glassy sample.

This work enhances the predictive capability of the NET-GP model by coupling it with a simple theory[38] capable of estimating the amount of swelling agent necessary to result in a transition from the glassy to the rubbery state based solely on the physical properties of the pure components. As the gas is absorbed, the polymer starts to swell, and eventually, as result of the augmented free volume, the glass transition temperature is lowered until the system crosses the transition point from glass to rubber. While the model obtained this way still requires independent information about the nonequilibrium dry polymer density, it does not make use of any specific adjustable parameter, and only equilibrium binary interaction coefficients need to be determined in order to perform the calculations.

In this paper, the predictions of the new model are compared with mass sorption data collected using a quartz crystal microbalance (QCM) and one-dimensional swelling data recorded using high-pressure ellipsometry (HPE) for PMMA/CO_2 films supported on silicon at two different temperatures and over a wide range of pressures. We also compare the modeling results with other literature data.

An additional significant finding of the present work is the experimental verification of the basic assumption of the NET-GP approach, never done before, which states that two different glassy polymer samples should exhibit the same behavior provided that their initial densities are the same, whatever their thermal, mechanical, and sorption histories.

This was achieved by preparing PMMA films with the same density using two completely different coating and curing techniques. These samples were used to collect sorption and swelling data as a function of pressure at two different temperatures using high-pressure ellipsometry (HPE) and quartz crystal microbalance (QCM) methods. HPE measurements yield data on the film thickness, which can be related to the film dilation through the expression

$$\% \text{ swelling} = \left(\frac{h - h_0}{h_0}\right) \times 100 \qquad (1)$$

HPE also provides information on the average refractive index of the swollen film, which can be converted into total carbon dioxide mass uptake[39,40] using the index of refraction of the pure components. In this work, the mass sorption measurements from HPE were compared to the more direct mass sorption data measured with QCM.

In the first part of this paper we describe the experimental procedures utilized in film preparation, swelling, and sorption measurements. This is followed by a description of the NET-GP model, the model used to predict the glass transition point, and the numerical procedure used for carrying out the sorption and swelling calculations. The last section presents the model results of the simulations along with the experimental results. The model performance has been tested at two different temperature, 35 and 50 °C, with pressures ranging from 0 to 1800 psi.

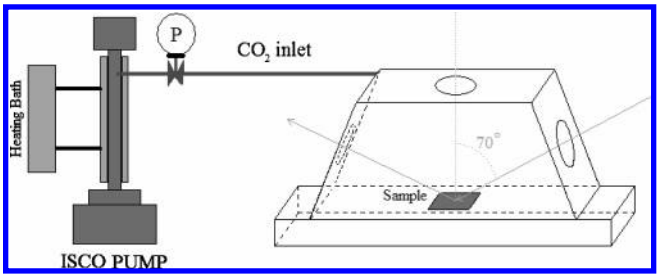

Figure 1. Experimental setup and ellipsometry high-pressure cell.

2. Experimental Methods

2.1. High-Pressure Ellipsometry (HPE). 2.1.1. Materials and Sample Preparation. PMMA (M_w = 72 kDa, M_w/M_n = 1.06) was purchased from Polymer Source, Inc., Dorval (Montreal, Canada). Toluene (Fisher) was used as solvent to dissolve PMMA. Silicon wafers (100 mm diameter, a ⟨100⟩ orientation) having ≈1.7 nm thick native oxide films (SiO_x) were purchased from International Wafer Services (Portola Valley, CA). The wafers were cleaned by soaking in a mixture of JTB-111 alkaline−surfactant, hydrogen peroxide, and DI water with a 4.6:1:22.8 volume ratio for 10 min and subsequently rinsed with copious amounts of DI water and dried with nitrogen. PMMA/toluene solutions were spin-coated onto silicon wafers using a Headway Research (model 131-024, Indianapolis, IN) spin-coater. The concentrations of the PMMA/toluene solutions and spin rates were varied to obtain films of different thickness. The coated wafers were annealed at 120 °C under vacuum for 3−6 h to remove any residual solvent. After spin-coating and annealing, the film thickness at room pressure was measured by ellipsometry (see below), and the initial mass was measured using a precision lab balance (Mettler Toledo, model AB204, Switzerland). Films of thickness ≈1.2 and ≈1.5 μm were formed with a resulting density of 1.187 g/cm^3. The densities of films used for HPE were matched as closely as possible to those used for QCM measurements. As described in detail below, the PMMA films for QCM experiments were formed by dip-coating QCM substrates into PMMA/toluene solution, followed by annealing in a vacuum at 80−90 °C for 1−2 h. The difference in density between the films used in QCM (1.189 g/cm^3) and those used in ellipsometry (1.187 g/cm^3) was less than 0.2%. The polymer mass per unit area on the QCM substrates was determined by measuring the fundamental frequency difference between the bare crystal and the coated crystal. SEM was used to measure the film thickness.

2.1.2. Ellipsometry Equipment. A variable angle spectroscopic ellipsometer (J.A. Woollam, Inc., Lincoln, NE) with rotating analyzer equipped with a custom-built high-pressure CO_2 cell was used in the HPE experiments. The angle of incidence (with respect to the sample normal) was fixed at 70°, and the wavelength was varied from 500 to 800 nm. The high-pressure cell, constructed of stainless steel, was equipped with three fused silica windows (2.54 cm in diameter and 1.5 cm in thickness, Rubicon Technology Franklin Park, IL) (cf. Figure 1). The two side windows were fixed at an angle of 110° from vertical in order to obtain normal incidence of the beam with the window to avoid any deviations that can cause a change in polarization of the light and to minimize the uncertainties in the incident angle of the beam on the sample. A custom-made copper sample holder with a spring clip was used to hold the wafer, and it was placed on the bottom of the cell. A torque wrench was used to put an equivalent and minimal amount

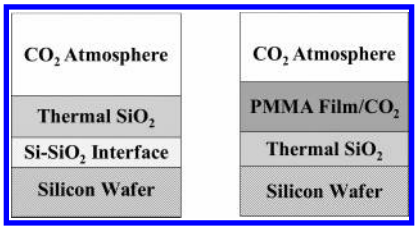

Figure 2. (a) Four-layer model used for wafer calibration. (b) Four-layer model used to analyze data for the swollen PMMA/CO_2 film.

of force to seal the windows to minimize the window birefringence induced by strain under high pressure. High-purity CO_2 gas (Matheson Gas Product, Montgomeryville, PA, purity > 99.999%) was charged to the cell to the desired pressure using an ISCO pump (model 260D, Isco, Inc., Lincoln, NE).

The pressure in the cell was measured using a pressure transducer (Omegadyne, model PX01C1-1KG10T, OMEGA Engineering, Inc., Stamford, CT) controlled to an accuracy of ±2 psi (0.14 bar). A heating tape was wrapped around the cell and was connected to a variable autotransformer (model 3PN1010, Staco, Hayward, CA) for temperature control. An insulation cap was used to cover the entire cell and heating tapes, except the windows, to obtain a uniform thermal equilibration that was found to be crucial in these experiments, especially near the critical point of CO_2. A custom-built metal heating plate was placed beneath the supporting stage to prevent heat losses. An ISCO pump (model 260D, Isco Inc., Lincoln, NE) was connected to a heated water bath (model 9110, Poly Science, Niles, IL) to preheat CO_2 to the desired temperature. The temperature inside the cell was measured by using a thermocouple (Omegadyne model HGKQSS-116G-12-OMEGA Engineering, Inc., Stamford, CT) and was controlled to within ±0.1 °C. The cell was allowed to reach thermal equilibration at each desired temperature for at least 1 h.

Birefringence of the windows can corrupt the polarization state of the light, and even nonbirefrigent windows can become birifrigent due to pressure-induced window strain.[41] This, in turn, can cause large errors in the calculated properties of the samples. An experimental procedure developed by J.A. Woollam Co., Inc., was used in this work to account for the effect of the window birefringence.[42,43]

2.1.3. Calibration at High Pressures. To test the effectiveness of the procedure for correcting induced window birefringence in the ellipsometric data, a calibration wafer (made at Triangle National Lithography Center) with a thick thermal oxide layer (≈85 nm) was used for scans at different pressures and temperatures. A four-layer model was used to fit the data (cf. Figure 2a). The refractive indices of the silicon substrate, the Si−SiO_2 interface layer, and SiO_2 were fixed using literature values.[44] The refractive index of the bulk CO_2 atmosphere at a given pressure and temperature was also obtained from literature values.[45,46] The ellipsometry data were fitted to determine the thickness of the thermal oxide layer and the angle of incidence using WVASE32 software (J.A. Woollam, Co. Inc.). Excellent fits to the experimental data were obtained when the effects of window birefringence were measured and accounted for in the model calculations. The maximum deviation of the measured thermal oxide thickness under pressure from the thickness of the oxide layer measured in ambient air without windows was found to range between −1 and + 4% over a range of pressures from 0 to 1800 psi.

2.1.4. Swelling Measurements. The PMMA films on the silicon wafer substrates were introduced into the chamber and scanned using the ellipsometer described above. The experimental ellipsometric data were fitted using a four-layer model, shown in Figure 2b, comprising the silicon substrate, a native oxide layer, a mixed polymer/CO_2 layer, and a bulk CO_2 medium. The refractive indices at different wavelengths were adopted from literature values[45,46] for silicon substrate, the native oxide, and the CO_2 atmosphere. The fitted parameters for the swelling experiments were the same as those in the calibration scan, with the additional fitting of the refractive index of the swollen PMMA/CO_2 layer. The refractive index of the swollen PMMA/CO_2 layer was modeled as a function of wavelength by assuming a Cauchy dispersion relationship.[47]

2.1.5. Mass Sorption Calculations Using Ellipsometry Data. Ellipsometry measurements provide values of the thickness and average refractive index of the swollen film. From this information it is possible to estimate the mass of gas absorbed given refractive index information for the pure components. Sirard et al.[40] showed that the mass concentration of CO_2 in a PMMA film can be estimated by applying the Clausius−Masotti equation[48,49] to each component in the swollen film

$$\frac{\langle n_j\rangle^2 - 1}{\langle n_j\rangle^2 + 2} = \frac{R_j}{M_{wj}}\rho_j = q_j\rho_j; \quad j = \mathrm{CO_2}, \mathrm{PMMA} \tag{2}$$

where $\langle n_j\rangle$ represents the average refractive index for CO_2 and for PMMA in the swollen layer over the wavelength range from 500 to 800 nm, R_j is the mole refraction, M_{wj} is the molecular weight, and ρ_j is the mass density of the component j. Equation 2 can be used to calculate values of the ratio R_j/M_{wj} for each component in the film, given literature values of the refractive indices of CO_2 and PMMA at the pressure and temperature in which the measurement is taken. The mass concentration of CO_2 and PMMA in the swollen PMMA film can be calculated from the measured refractive index $\langle n_f\rangle$ of the swollen film layer through the following mixing rule[39,40]

$$\frac{\langle n_f\rangle^2 - 1}{\langle n_f\rangle^2 + 2} = q_{\mathrm{CO_2}}\rho_{\mathrm{CO_2}} + q_{\mathrm{PMMA}}\rho_{\mathrm{PMMA}} \tag{3}$$

where q_{CO_2} and q_{PMMA} are determined from the pure component refractive index data.

In their analysis of sorption in glassy polymers using simple interferometry, Fleming and Koros have shown that the linear mixing rule in eq 3 may fail when the polymer is in the glassy state because of the difficulty of independently decoupling the thickness and the refractive index from optical data.[50] However, in our case, with the use of multiwavelength spectroscopic ellipsometry, it is possible to independently determine the thickness and the refractive index of a thin film, thus avoiding the aforementioned complications. Using this technique, HPE has been shown to be able to provide reasonably accurate estimates of sorption levels in rigid glassy polymers.[39]

A mass balance on the polymer may be used to relate the mass concentration of the polymer in the swollen film to the measured thickness change of the film upon swelling and the original polymer density

$$\rho_{\mathrm{PMMA}} = \rho^0_{\mathrm{PMMA}}\frac{h_0}{h} \tag{4}$$

Using eqs 2−4, the sorption of CO_2 can be estimated from knowing the quantities h, h_0, and $\langle n_f\rangle$ (mixture refractive index). The densities of PMMA were calculated, for temperature higher than the room temperature, using a thermal expansion coefficient[51] of 5.6×10^{-4} K^{-1}, and the refractive index of pure PMMA was measured by ellipsometry at 1 atm. The densities of CO_2 were taken[24] to be 0.94 at and 0.93 g/cm^3 at 35 and 50 °C, respectively. The refractive index of the CO_2 dissolved in the polymer was taken[45] to be 1.225 and 1.221 at 35 and 50 °C, respectively. Over the range of pressure of these experiments, the effect of pressure on the refractive index of both PMMA and CO_2 was negligible.

2.2. QCM Measurements. 2.2.1. Materials and Sample Preparation. 5.00 MHz AT-cut Si quartz crystals (a blank diameter of 8.5 mm and a thickness of 0.25 mm) were obtained from International Crystal Manufacturing (Oklahoma City, OK). The Si film was vacuum-sputtered over an Au electrode that provided the necessary electrical actuation to the quartz. The rms surface roughness of the crystals used was less than 10 nm (analyzed using AFM). The crystal was connected to a voltage-controlled oscillator (Maxtek model PLO-10, Santa Fe

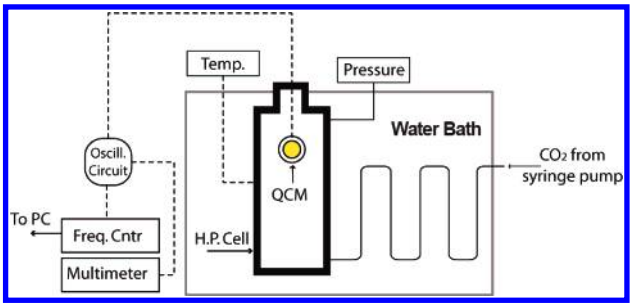

Figure 3. Schematic diagram of the QCM apparatus

Springs, CA). This oscillator provides two outputs: frequency and voltage. The voltage reading is inversely proportional to the resistance of the crystal. The oscillator is further connected to an Agilent 225 MHz universal frequency counter (model 53131A, Palo Alto, CA) that records the frequency of the vibrating crystal. The time-dependent frequency readings were stored on a computer using Agilent Intuilink Connectivity software.

PMMA films for the QCM experiments were cast onto the surface of the crystal by dip-coating. The crystal was dipped vertically into a 2.4 wt % PMMA/toluene solution, allowed to equilibrate for a specific time, and then was withdrawn from the solution at a controlled rate using a motorized device. The coated crystal was dried under vacuum at 80−90 °C for 1−2 h. The clean crystal was then placed in the cell under vacuum (0.01 psia), using precision DD-20 (Inxs Inc. Delray Beach, FL) vacuum pump, and the fundamental frequency F_0 of the coated crystal was recorded. The stable frequency level is indicative of complete evaporation of the solvent from the polymer during curing. The value of the stabilized frequency of the coated QCM in a vacuum was utilized to calculate the mass of coated polymer by comparing to fundamental frequency of the quartz crystal without polymer. The annealing conditions were chosen so that the density of the films formed for the QCM samples were as close as possible to the density of the films made for the ellipsometry experiments (final measured value 1.187 g/cm^3 for the ellipsometry sample and 1.189 g/cm^3 for the QCM sample).

2.2.2. High-Pressure QCM Cell. The custom-built pressure cell consists of a thick-wall stainless steel cylinder (63.5 mm i.d. × 200 mm height), with a high-pressure electrical feedthrough (Conax Buffalo Technologies, NY) at the top end to drive the QCM (cf. Figure 3). The cell has an inside volume of 25 cm^3 and a maximum working pressure of 7500 psi. The crystal was placed in the cell and connected to the oscillator through the electrical feedthrough during an experiment. A high-pressure thermocouple (Omega, Stamfortd, CT) was placed in the cell to monitor the temperature of the CO_2 fluid. Data acquisition was accomplished via a National Instrument DAQ interface using Labwiew software. The whole assembly was then placed in a custom-built water bath and controlled to within ±0.1 °C.

2.2.3. Mass Sorption Measurements. QCM crystals coated with polymer films were placed in the pressure cell, and the fundamental F_0 frequency of the QCM was measured in a vacuum. After a stable signal was achieved, CO_2 was slowly introduced into the chamber to increase the pressure. The frequency was then allowed to reach a new stable level and recorded. This procedure was repeated for the third pressure level, and so on. A pressure range from 0 up to 1800 psi was examined in steps of 150 psi. After the time-dependent frequency readings were recorded for each pressure, an analysis was performed in order to obtain the correspondent mass of CO_2 uptake vs time behavior.

The frequency of the QCM can be affected by several factors, including the mass adsorbed on the crystal surface (m), the pressure (P), the properties of the surrounding medium, and the temperature (T). Since the temperature was held constant during these experiments, the total change in frequency can be written as the sum of the contributions from mass adsorbed, pressure, and the surrounding medium[52,53]

$$\Delta F = F - F_0 = \Delta F_m + \Delta F_P + \Delta F_\eta \tag{5}$$

Estimation of the mass effect can be done using the well-known Sauerbrey equation[54−58]

$$\Delta F_m = -2F_0^2 \Delta m/(\mu_q \rho_q)^{1/2} = -C_m \Delta m \tag{6}$$

where C_m is the mass sensitivity constant (56.6 μg/cm^2),[52] F_0 is the fundamental frequency of the crystal, Δm is the mass per unit area absorbed on the crystal, and the quantities μ_q and ρ_q are the shear modulus and density of the quartz, respectively. The equation above represents a simple linear relationship between the change in frequency and the mass uptake. For a crystal coated with a viscoelastic polymer layer this simple relationship may not hold. However, the extent of the deviation from eq 6 depends strongly upon the film thickness. Analysis on this subject in the literature has shown that the linear approximation can be used with confidence only when the load on the QCM is small, i.e., when the film thickness is small (less than a few micrometers).[55−58] In our experiments, all the film thickness values were on the order of 1 μm, easily justifying the use of eq 6 in calculating the change in frequency due to mass sorption. The QCM sorption data agreed extremely well with prior work in the literature, providing additional proof of the accuracy of eq 6 in this application.

As for the second term, Stockbridge[59] found that the frequency changes linearly with pressure

$$\Delta F_P = C_P P \tag{7}$$

where C_P is a constant. This relation has been tested previously[52,53] and found to be valid for the crystals used in this work. The value of C_P was found to be ∼0.34 Hz/psi in the range of temperature considered here for a 5 MHz quartz crystal.[52]

The viscosity contribution it is more difficult to quantify. Kanazawa and Gordon proposed the following equation for the oscillation frequency of a quartz resonator in contact with fluid[60]

$$\Delta F_\eta = -F_0^{3/2}\left(\frac{\rho_f \eta_f}{\pi \rho_q \mu_q}\right)^{1/2} \tag{8}$$

where ρ_f and η_f denote the density and shear viscosity of the fluid medium surrounding the crystal. It should also be noted that in these experiments the initial conditions were chosen to be in a vacuum, so that P, ρ_f, and η_f are used rather than ΔP, $\Delta\rho_f$, and $\Delta\eta_f$.[52,53]

Although this relation has been used previously to perform similar calculations in the case of bare crystal,[52] it should be recognized that the presence of the polymer film introduces a discontinuity in the viscosity profile in the vicinity of the QCM surface. However, since the polymer film thickness is much smaller than that of the quartz (≈0.1%), this relation provides a good approximation to account for the viscosity effect.

3. Theory

3.1. The NET-GP Model. This section summarizes the NET-GP model for sorption of gases into glassy polymers for the case of homogeneous, amorphous, and isotropic materials.[34−37] The model makes use of the well-known concept of order parameter for the description of the nonequilibrium state of the glassy phase at a given temperature, pressure, and composition. This idea provides a useful framework for describing systems that are not at equilibrium and avoids the introduction of mathematically cumbersome memory functions otherwise necessary for dealing with sample histories. The model then assumes that an unambiguous description of the thermodynamic properties of the glassy polymer−gas mixture can be based on a set of state variables in

which, along with temperature T, pressure P, and gas content ω_1, the polymer mass density ρ_2 is included as independent variable which measures the volume deformation of the polymer network

$$\Sigma = \Sigma(T,P,\omega_1,\rho_2) \tag{9}$$

Thus, any specific nonequilibrium function F^{NE} of the state of the system can be described by an expression of the form

$$F^{NE} = F^{NE}(T,P,\omega_1,\rho_2) \tag{10}$$

With this assumption, polymeric samples below the glass transition temperature have identical thermodynamic properties at given T, P, and ω_1, provided the order parameter ρ_2 is the same, regardless of their thermal, mechanical, or and sorption histories. Indeed, while the use of a single order parameter may not be sufficient to describe all the nonequilibrium characteristics of the structure of a glassy polymer mixture,[61,62] the first-order approximation used in NET-GP addresses the major effect of volume deformation on the properties of the glassy polymeric mixture, and it allows for a quantitative representation of sorption behavior which is satisfactory for most technical purposes.

The thermodynamic analysis of NET-GP model relies on the additional assumption that the order parameter ρ_2 is an internal state variable for the system; i.e., its rate of change in time depends strictly on the state of the system:

$$\frac{d\rho_2}{dt} = f(T,P,\omega_1,\rho_2) \tag{11}$$

While different order parameters can be used to describe the same thermodynamic properties of a glassy gas−polymer mixture, the assumption of different internal state variables definitely leads to different expressions for the properties in the nonequilibrium states. In this sense, results of the NET-GP model are unique with regard to earlier attempts to describe properties of glassy phases by means of different order parameters.[30−32]

Given the assumptions of eqs 10 and 11, through the use of well-established tools of thermodynamics of systems endowed with internal state variables, the following conditions hold for the nonequilibrium Helmholtz free energy density a^{NE} and penetrant chemical potential μ_1^{NE} in the mixture:[35−37]

$$a = a^{NE}(T,P,\omega_1,\rho_2) = a^{EQ}(T,\omega_1,\rho_2) \tag{12}$$

$$\mu_1^{NE} = \left(\frac{\partial a^{NE}}{\partial n_1}\right)_{T,n_2,\rho_2} \tag{13}$$

Equations 12 and 13 constitute the key results of the thermodynamic analysis of nonequilibrium states for penetrant−polymer mixtures below the glass transition temperature. They allow for the derivation of expressions for the free energy and solute chemical potential of any nonequilibrium state of a glassy gas−polymer mixture, once reliable expressions for the corresponding equilibrium conditions are known. It is thus possible to calculate the solute solubility in the system, knowing the polymer mass per unit volume, through the classical phase equilibrium condition

$$\mu_1^{(S)}(T,P,\omega_1,\rho_2^{\infty}) = \mu_1^0(T,P) \tag{14}$$

or, equivalently, in terms of fugacities

$$f_1^{(S)}(T,P,\omega_1,\rho_2^{\infty}) = f_1^0(T,P) \tag{15}$$

In the expressions above, μ_1^0 and f_1^0 are the equilibrium chemical potential and fugacity of a pure penetrant phase, at temperature T and pressure P, respectively, and ρ_2^{∞} is the pseudo-equilibrium polymer density the system reaches under sorption conditions. It is important to stress that ρ_2^{∞} must be known without using equilibrium arguments in order to solve eqs 14 and 15 for the pseudo-equilibrium gas content ω_1.

In a low-pressure sorption experiment, the swelling induced by the penetrant is negligible, and the pseudo-equilibrium value of the density, ρ_2^{∞}, can be approximated by the initial density of the pure polymer ρ_2^0. It is useful to remember that ρ_2^0 is a nonequilibrium property which depends on the history of the polymeric material, and as such it should be specifically calculated for the case of interest. The problem of representation of solubility isotherms in the low-pressure range has been addressed in previous papers, where numerous examples have been discussed.[35−37,63] However, in the more general case, the polymer density ρ_2^{∞} changes with penetrant pressure P in the external phase, and its variation must be considered in order to correctly describe sorption isotherms at moderate and high pressures.

Careful analysis of experimental dilation data for a wide variety of systems indicates that at constant temperature the pseudo-equilibrium polymer density varies linearly with pressure,[64] so that it can be adequately represented by an equation of the form

$$\rho_2^{\infty}(P) = \rho_2^0(1 - k_s P) \tag{16}$$

where the parameter k_s is the dilation coefficient of the polymeric material in the gaseous atmosphere. This is also a nonequilibrium variable, which may change according to the thermal and sorption history of the polymeric material, as well as depending on sorption/desorption runs. Figure 4 shows a schematic representation of the density behavior with pressure at constant temperature. An increase in pressure results in a linear decrease in density until a certain pressure P_g is reached at which the amount of solvent absorbed is sufficient to reach the glass transition concentration ω_1^g at which the equilibrium behavior is recovered. The point (P_g,ρ_2^g) is the glass transition point, and for a given mixture it depends only on temperature.

The case of representing sorption isotherms in glassy polymers up to moderate pressures, in which the swelling effect of the penetrant component must be taken into account, has been considered in a previous work through the discussion of several examples.[64] However, while the dilation coefficient k_s has a precise physical meaning, it has been treated in this previous work as an adjustable parameter that needed to be fitted using high-pressure nonequilibrium solubility data. In the following section, an approach is presented that eliminates this shortcoming present in earlier NET-GP theories.

3.2. Model for Plasticization. Using classical and statistical mechanical arguments, Chow[38] derived a

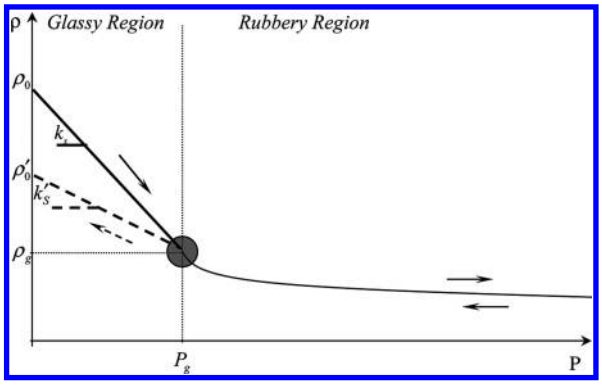

Figure 4. Schematic linear behavior of the polymer density with pressure at constant temperature in the glassy region.

Table 1. Physical Properties of Un-Cross-Linked and Nonbranched PMMA[65,66]

$z = 2$	$\Delta C_p = 32.72$ J/(mol K)
$M_p = 100.12$ kg/mol	$T_g = 105$ °C
$M_d = 44$ kg/kmol	

relationship expressing the depression of the glass transition temperature of a polymer−solvent mixture (T_g^{mix}) by means of liquid plasticizers at low pressures, in terms of the glass transition temperature (T_g^0) of the pure polymer, the excess heat capacity, and the mass fraction of solvent inside the polymer. The derivation was based on the application of the Gibbs−DiMarzio criterion, which states that at the glass transition temperature the entropy is zero, to a lattice model.

The resulting expression for the glass transition temperature of the polymer−solvent mixture is given by

$$\ln\left(\frac{T_g^{mix}}{T_g^0}\right) = \Psi[(1-\theta)\ln(1-\theta) + \theta \ln \theta] \quad (17)$$

with

$$\Psi = \frac{zR}{M_p \Delta C_p} \quad (18)$$

and

$$\theta = \frac{M_p}{zM_d}\frac{\omega_1}{1-\omega_1} \quad (19)$$

In the equations above, T_g^0 is the glass transition temperature of the dry polymer, and M_p and M_d are the molecular weights of the monomer and solvent, respectively. The quantity ΔC_p represents the difference in heat capacity between the supercooled liquid and glass, z is the lattice coordination number, R is the ideal gas constant, and ω_1 is the mass fraction of solvent in the polymer. In Table 1 these parameters, obtained from the literature,[65,66] are listed for PMMA.

Chow's theory requires that the dimensionless parameter θ in eq 19 be always less than 0.25 (small concentration limit).[38,67] In the present work, the most extreme case has been represented by the lower temperature, where a carbon dioxide mass fraction of 0.146 is needed to lower the glass transition temperature to 35 °C. This, in turn, corresponds to a value of $\theta = 0.194$, well within the window of applicability of eq 17.[38,67]

Since eq 17 was developed for calculating the glass transition point in the presence of a liquid plasticizer, it does not have any dependence on pressure. In our case the plasticizer is a high-pressure gas and increases in pressure beyond the critical point may compress the polymer sample, reducing the free volume and increasing its glass transition temperature. However, the effect of pressure on most polymers only becomes important at pressures far above 500 bar,[33] significantly above the pressures being considered in this work. As a result, it is reasonable to neglect pressure effects on the glass transition temperature and to use eq 17 in the calculations of the depression of the glass transition temperature for the PMMA/CO_2 system.

A version of the Sanchez−Lacombe equation of state has been developed recently to address the problem of sorption in glassy polymers that also provides a method for estimating the glass transition depressiondue to sorption.[33] Condo et al. have shown that the Chow theory provides a better quantitative agreement with experimental data[67] than this new Sanchez−Lacombe theory. Our own calculations (not shown here) have also confirmed the results of Condo et al., showing that the Chow theory led to a much better fit to T_g data, especially at high solute concentrations. Because of its simplicity and better predictive capability, the Chow model was used here to make all predictions of T_g values. Just as the NET-GP theory can be used with any equilibrium equation of state, the Chow theory can be readily implemented with any equilibrium thermodynamic model to predict glass transition temperatures.

3.3. Calculation of Solubility Isotherms in Glassy Polymers. Equations 17−19 make it possible to find the value of the penetrant composition that causes the glass transition temperature to drop down to the experimental temperature. Knowing this value, it is possible to calculate, using the equilibrium equation of state, the value of pressure and polymer density at the glass/rubber transition point (P_g,ρ_2^g). The assumption that the density variation with pressure is approximately linear up the glass transition point leads to the expression

$$\rho_2^\infty(P) = \rho_2^0 + P/P_g(\rho_2^g - \rho_2^0) \quad (20)$$

where ρ_2^g can be evaluated using the equilibrium EoS at T, P_g, and ω_1^g. Knowing the density at the glass−rubber transition, it is possible to calculate the swelling parameter combining eqs 16 and 20

$$k_S = \frac{1}{P_g}\left(1 - \frac{\rho_2^g}{\rho_2^0}\right) \quad (21)$$

The knowledge of the initial polymer density is crucial for the present model; however, in many cases in the literature this information is not provided, either because it is not deemed to be relevant or because it is difficult to measure the given size or shape of the sample. For those cases in which it is not directly available, we figured out a simple procedure to estimate its value from swelling data.

Taking as example swelling data from the works of Wissinger et al.[68] and Zhang et al.,[32] Figure 5 presents the swelling information as a density ratio (ρ_2/ρ_2^0) depicting the variation of PMMA density with CO_2 pressure at two different temperatures, 32.7 and 35 °C. From the slope of the line it is possible to evaluate the value of k_s, and then by using eq 21 and knowledge

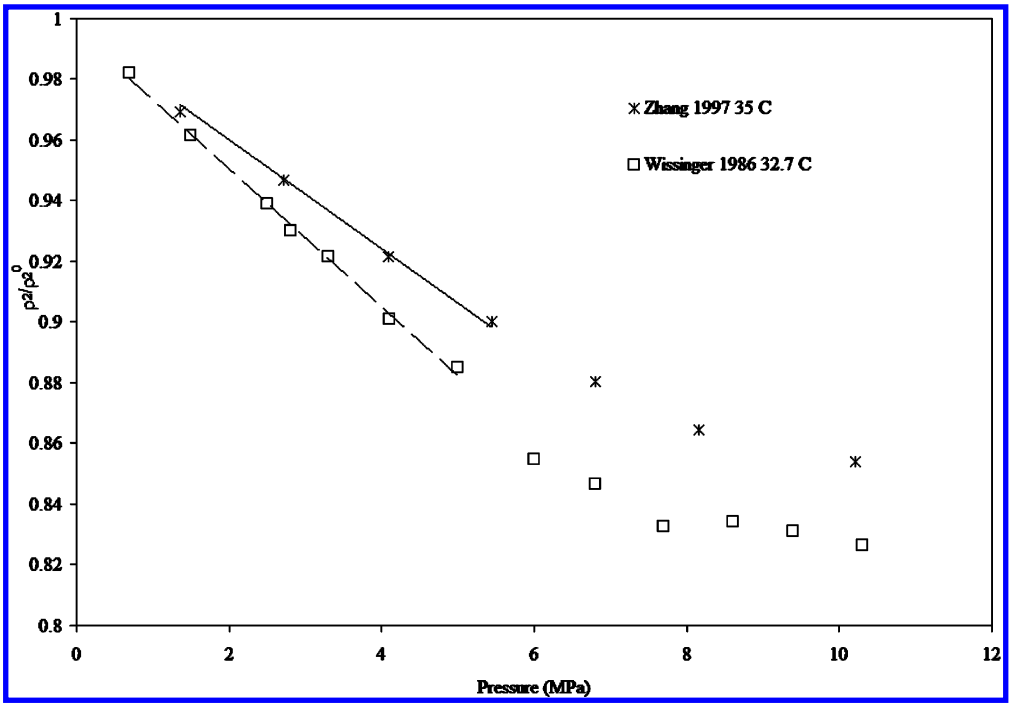

Figure 5. Linear behavior of PMMA density with CO_2 pressure in the glassy state.[32,61]

about the glass transition point (P_g,ρ_2^g) one can estimate to a good approximation the initial polymer density ρ_2^0.

A general procedure for the calculation of the pseudo-equilibrium penetrant fraction for vapor or gas sorption in glassy polymers at an assigned temperature and pressure can now be stated as follows:

- Choose a suitable equation of state (EoS) for the penetrant/polymer pair that provides a successful description of system properties in the melt or rubber phase.
- Choose a model for calculating either the chemical potential or the fugacity of penetrant in the gaseous phase. In most cases the same model could be conveniently used to represent thermodynamic properties in both the polymeric and gaseous phases.
- If not available, estimate the mass density of the pure polymer at the initial T and pressure of interest.
- Evaluate the glassy/rubbery transition point (T,ω_1^g) by taking $T_g^{mix} = T$ in eq 17 and by solving iteratively for ω_1^g. By using the equilibrium equation of state at constant T, the mixture density and the mass fraction of the penetrant at a given P, $\omega_1(P)$, can be calculated. The glass transition pressure is defined as the pressure at which the mass fraction of penetrant becomes equal to ω_1^g; this fixes the point (P_g,ρ_2^g). Finally, evaluate the polymer density in the penetrant polymer mixture according to whether the pressure is above or below the glass transition pressure

$$\rho_2 = \begin{cases} \rho_2^{\infty} & \text{from eq 19} \quad \text{for } P < P_g \\ \rho_2^{eq} & \text{from EoS} \quad \text{for } P \geq P_g \end{cases} \tag{22}$$

- For each pressure value solve either eq 14 or 15 for the penetrant density in the polymeric mixture.

3.4. Equilibrium Equations of State. According to the general procedure described above, different thermodynamic models can be derived for sorption and swelling in glassy polymers using different expressions for the description of polymer/penetrant mixture properties in the melt phase. This makes the NET-GP approach highly flexible since it can be used with any equilibrium EoS capable of describing accurately the melt or rubbery phase.

This work focuses on one of the most successful and frequently used equations of state for polymer solutions, the Sanchez−Lacombe equation of state (SL).[69−71] The SL EoS is a lattice-fluid model, in which each component is divided into parts (or "mers") that are placed into a lattice and are allowed to interact with a mean-field intermolecular potential. In the SL EoS, the reduced density is related to the reduced pressure and temperature according to

$$\tilde{\rho}^2 + \tilde{P} + \tilde{T}\left[\ln(1-\tilde{\rho}) - \left(1 - \frac{1}{r}\right)\tilde{\rho}\right] = 0 \tag{23}$$

The compressibility of the system and the expressions for the fugacity coefficient, derived from the residual Helmholtz free energy,[71,72] are

$$Z = \frac{\tilde{P}\tilde{v}}{\tilde{T}}\, r \tag{24}$$

$$\ln \varphi_i = -\ln Z + (Z-1) + \left(\frac{\partial a^{res}(T,V,n)}{\partial n_i}\right)_{T,V,n_j} \tag{25}$$

$$\ln \varphi_i(T,P,\omega_i) = -\ln Z + (Z-1) + r_i\left[-\frac{\tilde{\rho}}{\tilde{T}} + \left(\frac{1}{\tilde{\rho}} - 1\right)\ln(1-\tilde{\rho}) + 1\right] + \left(\frac{Z-1}{r}\right)\left[\frac{nr}{v^*}\left(\frac{\partial v^*}{\partial n_1}\right)_{n_j}\right] - \frac{\tilde{\rho}}{\tilde{T}}\left[\frac{nr}{\epsilon^*}\left(\frac{\partial \epsilon^*}{\partial n_1}\right)_{n_j}\right] \tag{26}$$

In this work two versions of the SL equation of state have been used. The first version (SL-I)[69−71] is the classical version with one adjustable binary parameter in the mixing rules, as expressed by eqs 27−29. The second version (SL-II) has two adjustable binary pa-

Table 2. Pure Component Parameters[33,72]

pure parameter[33−72]	CO_2	PMMA
T^* [K]	283	696
P^* [MPa]	659	503
ρ^* [g/cm^3]	1.62	1.269

Table 3. Interaction Parameters for Both Versions of the SL Equation of State[a]

binary parameters	SL-II	SL-I
k_{ij}^{35}	0.1246	−0.044
η_{ij}^{35}	0.033	
k_{ij}^{50}	0.1161	−0.040
η_{ij}^{50}	−0.015	

[a] Parameters fit to sorption data above 100 bar at two temperatures, 35 and 50 °C.

rameters in the mixing rules as proposed more recently by McHugh and Krunokis,[1,71−73] as represented by eqs 29−32.

$$v^* = \sum \phi_i v_{ii}^* \tag{27}$$

$$\epsilon^* = \sum\sum \phi_i \phi_j \epsilon_{ij}^* \tag{28}$$

$$\epsilon_{ij}^* = \sqrt{\epsilon_{ii}^* \epsilon_{jj}^*}(1 - k_{ij}) \tag{29}$$

$$\epsilon^* = \frac{1}{v^*}\sum\sum \phi_i \phi_j (v\epsilon)_{ij}^* \tag{30}$$

$$v_{ij}^* = \frac{1}{2}(v_{ii}^* + v_{jj}^*)(1 - \eta_{ij}) \tag{31}$$

$$v^* = \sum\sum \phi_i \phi_j v_{ij}^* \tag{32}$$

For a complete description of the symbols used above the reader is referred to the notation section at the end of the paper.

In the following section, results from the correlation of experimental sorption and swelling data for the PMMA/CO_2 system through use of NET-GP model will be shown in detail, using both the SL-I and SL-II equations of state. The pure component parameters for CO_2 and PMMA for use in the SL-I and SL-II equations of state were obtained from the literature and are tabulated in Table 2. The critical point for carbon dioxide predicted using these parameters is (42 °C, 75 bar), which means that the model overestimates the critical temperature by about 11 °C and overestimates the critical pressure by only 20 psi. In the case of the lowest temperature considered in this study, the CO_2 model will predict a phase change from gas to liquid instead of the real transition from gas to supercritical CO_2. The binary interaction parameters, k_{ij} for SL-I and the pair (k_{ij}, η_{ij}) for the SL-II model, were determined by fitting the EoS to sorption data at pressures above 100 bar. In this region the PMMA/CO_2 mixture is rubbery, and the SL equation of state is able to do an excellent job of correlating the thermodynamic properties. Table 3 lists values of the binary interaction parameters for SL-I and SL-II taken from high-pressure data at 35 and 50 °C. The values of these parameters are in general agreement with previous literature results.[73] The data used to make these parameter fits are presented Figures 7−9, to be discussed in detail in the following section. Once the binary interaction parameters were estimated, the model was used to compute sorption and swelling behavior over the entire range of pressure including the glassy region using the NET-GP approach described above.

4. Results and Discussion

To provide good estimates of the effect of the penetrant concentration on the glass transition pressure, the modified NET-GP procedure described above must result in good estimates of the dilation parameter. Table 4 compares experimental[64] and predicted values for the swelling coefficient k_s for a series of polymer−gas pairs. All the reported values were calculated at 35 °C. The predicted values of k_s were obtained using the procedure described above, using eq 21 coupled with the SL-II equation of state with pure component and binary interaction parameters fitted in this work for the PMMA−CO_2 pair and taken from the literature for the other pairs.[64,65] The predicted swelling coefficients are all within 1−4% of the experimental values, indicating that the procedure is indeed capable of making reasonable extrapolations of the density variations with pressure at constant temperature.

Solubility data obtained for CO_2 in PMMA at 50 °C as measured by both the HPE and QCM techniques in sorption/desorption experiments are compared in Figure 6a, where the quantity Ω_{CO_2} represents the ratio of grams of CO_2 absorbed per gram of polymer (g_{CO_2}/$g_{polymer}$).

The two series of measurements are in very good agreement with each other, except for a few scattered points at low pressures. At this relatively high temperature there is very little hysteresis in the CO_2 isotherm as the pressure is decreased. As discussed in the experimental description, films prepared for QCM and HPE followed two completely different preparation histories but have nearly identical densities. The excellent agreement between the sorption data for both samples shown in Figure 6a indicates not only that the two measurement techniques are highly consistent but also that glassy polymer films prepared according to two completely different protocols exhibit similar sorption behaviors, provided they are characterized by the same polymer mass density. This result provides experimental verification of one of the basic assumptions in the development of NET-GP models, namely, that the glass polymer density can be used as a single order parameter to determine swelling and sorption, and as a consequence, samples with the same initial density are expected to exhibit similar sorption and swelling behavior regardless of their past histories. This is the first experimental verification of the suitability of this assumption.

HPE can provide a prompt measurement for the glass transition pressure, i.e., the pressure required to have sufficient amount of CO_2 absorbed into the polymer matrix necessary to lower the glass transition temperature to the experimental temperature.[39,74] To determine the glass transition pressure, we measured the ellipsometric angle ψ as a function of CO_2 pressure at different wavelengths (from 500 to 800 nm) for both sorption and desorption isotherms. Figure 6b shows a plot of the average ψ values as a function of pressure along with straight line fits to point out the difference in slopes before and after the critical pressure. The pressure at which the change in curvature occurs is

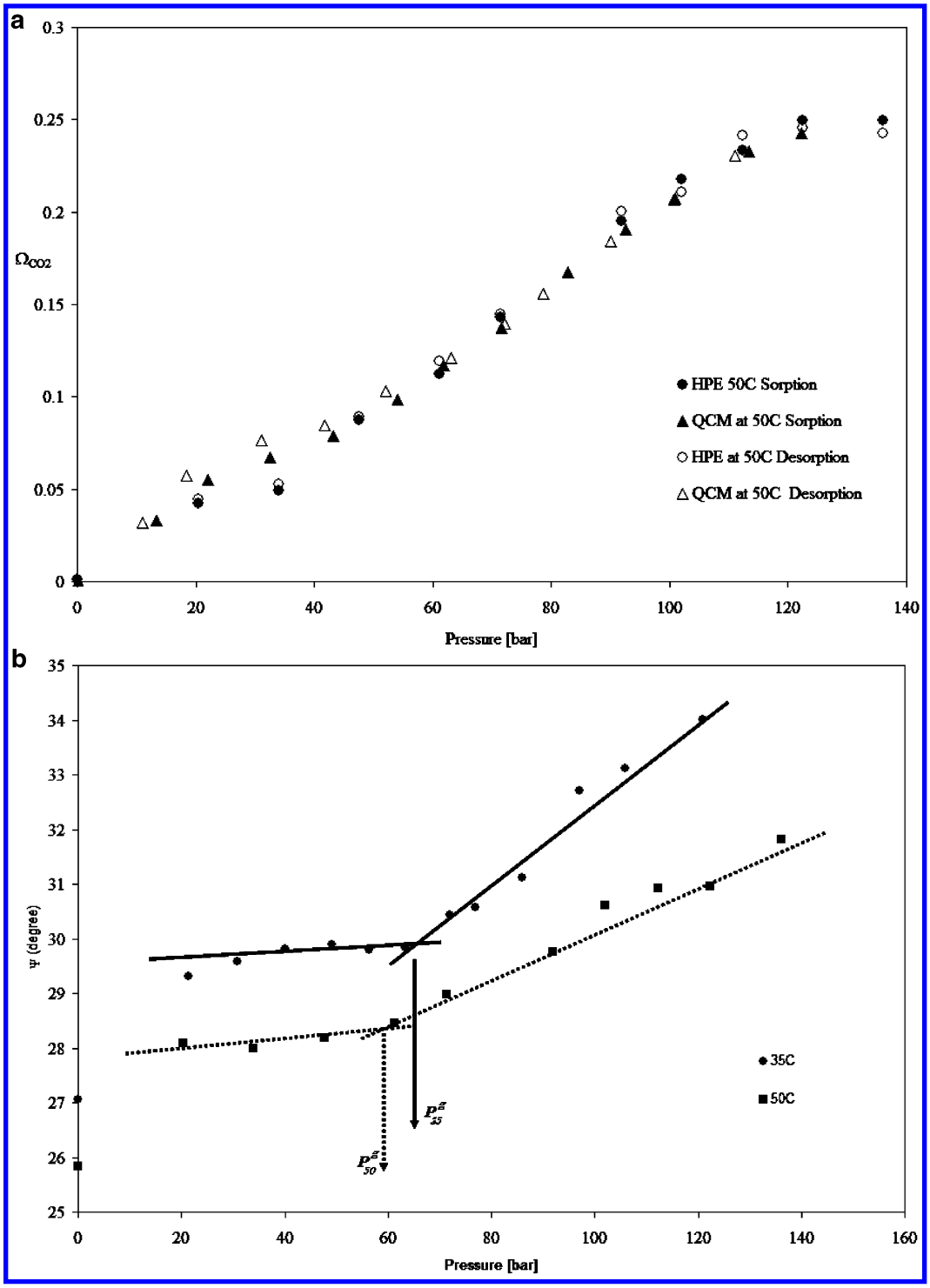

Figure 6. (a) Solubility isotherm for CO_2 in PMMA at 35 °C from sorption and desorption experiments as measured by QCM and high-pressure ellipsometry. (b) Ellipsometric angle ψ as a function of CO_2 pressure at 35 and 50 °C. The CO_2-induced glass transition pressure, P_g, is identified as the pressure at which the slope of the $\psi-$pressure curve changes.

identified as the P_g,[74] i.e., $P_g^{35} \cong 64$ bar and $P_g^{50} \cong 58$ bar, which are in very good agreement with previous measurements.[74,75] The beginning of the hysteresis in the dilation data upon sorption and desorption cycles has been often associated with the the glass transition pressure.[39,40] The data in Figure 6a,b indicate that the P_g values estimated from the change in slope of the ellipsometric angle agree quite well with P_g values estimated from the presence of hysteresis in dilation during the sorption and desorption cycles.

Figure 7a shows experimental data for CO_2 solubility in PMMA at 50 °C measured from QCM sorption experiments. Superimposed on the data in Figure 7a are the predictions of the NET-GP model using the SL-I and SL-II equations of state. The interaction parameters used in the SL-I and SL-II models fitted to the sorption data for pressures greater than 100 bar are listed in Table 3. According to the Chow theory in eq 17, the CO_2 concentration at the glass transition point should correspond to a value of $\Omega_{CO_2}^{50} = 0.096$. At this penetrant concentration, the glass transition pressure P_g^{50} was estimated as 46 and 54 bar using the SL-I and SL-II models, respectively, within a few bars from the mea-

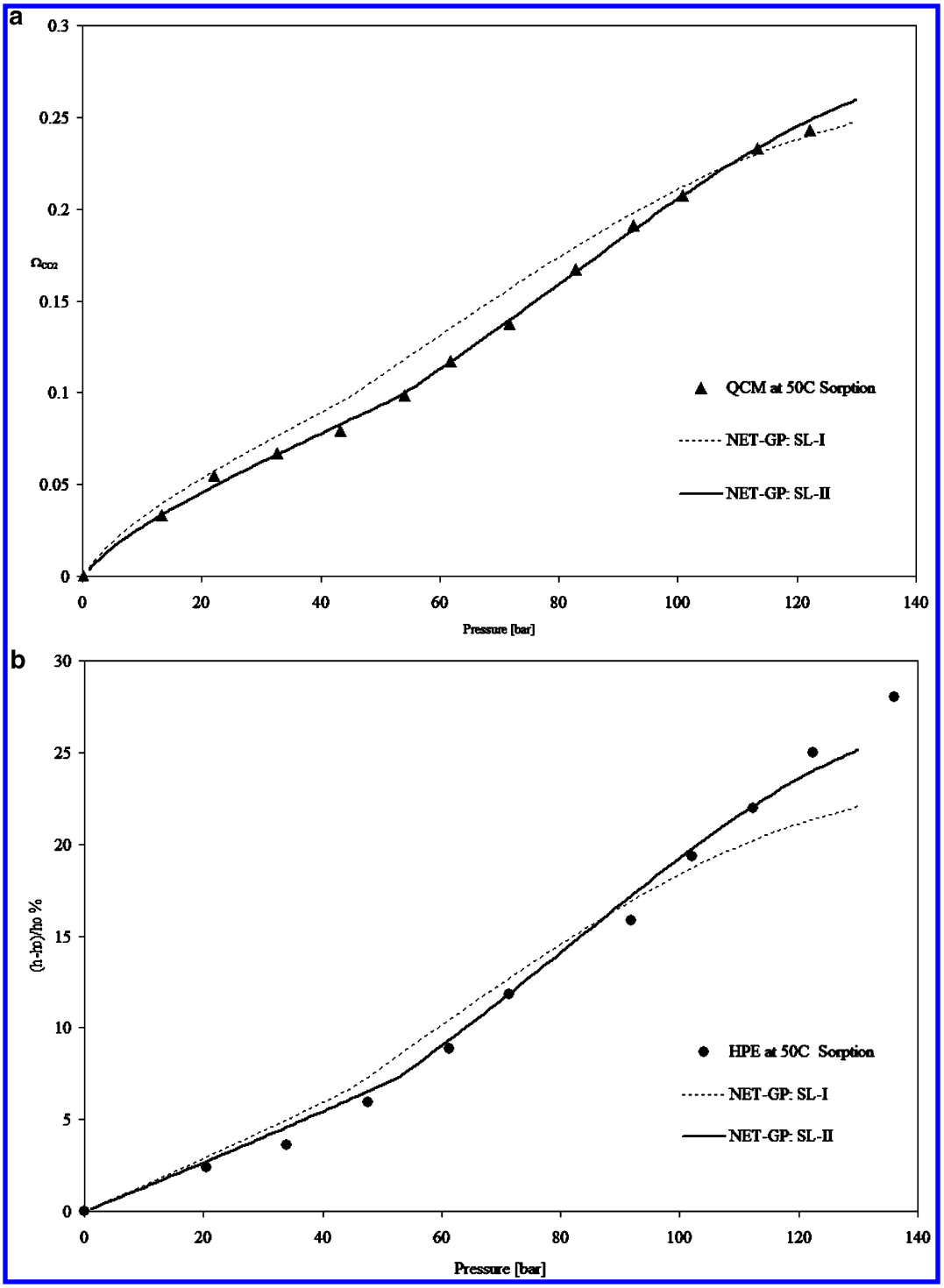

Figure 7. (a) Solubility isotherm for sorption of CO_2 in PMMA at 50 °C: comparison between experimental data and fitting results using NET-GP SL-I [thin solid line] and NET-GP SL-II [thick solid line]. (b) Volume swelling isotherm for sorption of CO_2 in PMMA at 35 °C: comparison between experimental data and predicted results using NET-GP SL-I [thin solid line] and NET-GP SL-II [thick solid line].

sured experimental value. Model predictions below P_g shown in Figure 7a were obtained from solubility calculations using the nonequilibrium NET-GP approach with the SL-I and SL-II equations of state. Solubility results obtained with NET-GP and the SL-II equation of state exhibit a clear representation of all features shown by experimental data over the entire pressure range, including a slight change in the slope at the glass transition pressure. A less accurate picture of solubility and pseudo-solubility data is obtained by means of NET-GP with the SL-I equation of state, although the qualitative variation of the solubility isotherm with pressure range is correctly represented.

Figure 7b shows % swelling or dilatation data using HPE during sorption at 50 °C for PMMA at CO_2 pressures corresponding to the sorption data shown in Figure 7a. The predicted % swelling results from the NET-GP model using SL-I and SL-II parameters shown in Table 3 are superimposed on the experimental results. The swelling calculations shown in this figure did not require any additional fits of

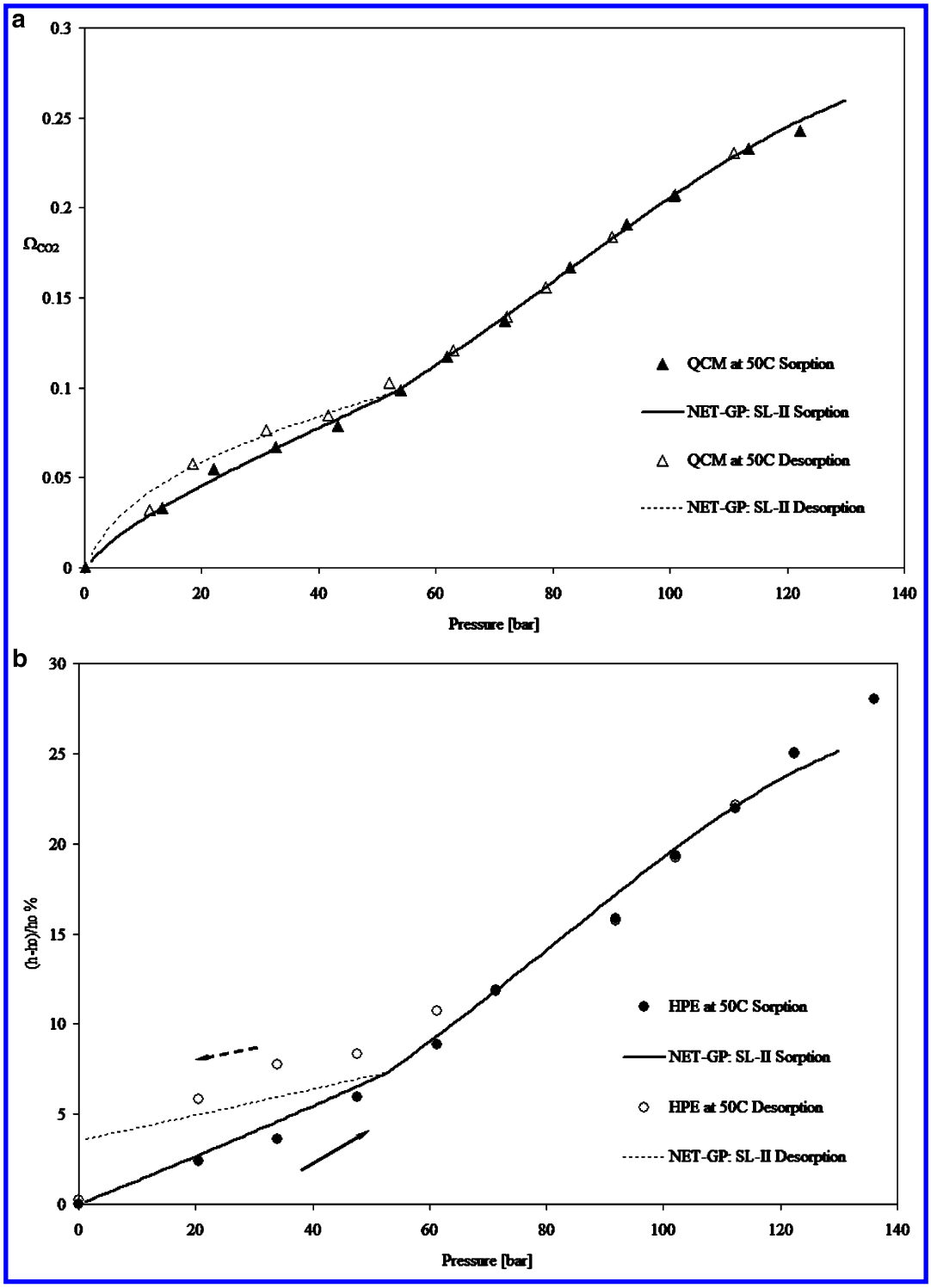

Figure 8. (a) Solubility isotherm for sorption−desorption cycle of CO_2 in PMMA at 50 °C: comparison between experimental data and fitting results using the NET-GP SL-II theory. (b) Volume swelling isotherms for sorption−desorption cycle of CO_2 in PMMA at 50 °C: prediction using the NET-GP SL-II theory.

parameters, only a direct application of the parameters fitted in the high-pressure regime with sorption data shown in Figure 7a. As was the case with the sorption data, the results from the NET-GP approach with the SL-II model provide a more accurate representation of the swelling experimental data. Considering that all the model results in Figure 7b were complete predictions, even the less accurate NET-GP SL-I model resulted in an impressively good comparison with the % swelling experimental results. The linear behavior assumed for volume swelling below P_g^{50} in eq 16 is clearly visible in the model predictions, and it is substantially confirmed by the experimental data.

Having established that the NET-GP SL-II model clearly offers a more accurate representation of the experimental results for the PMMA/CO_2 system, only the results of this model will be presented in subsequent discussions.

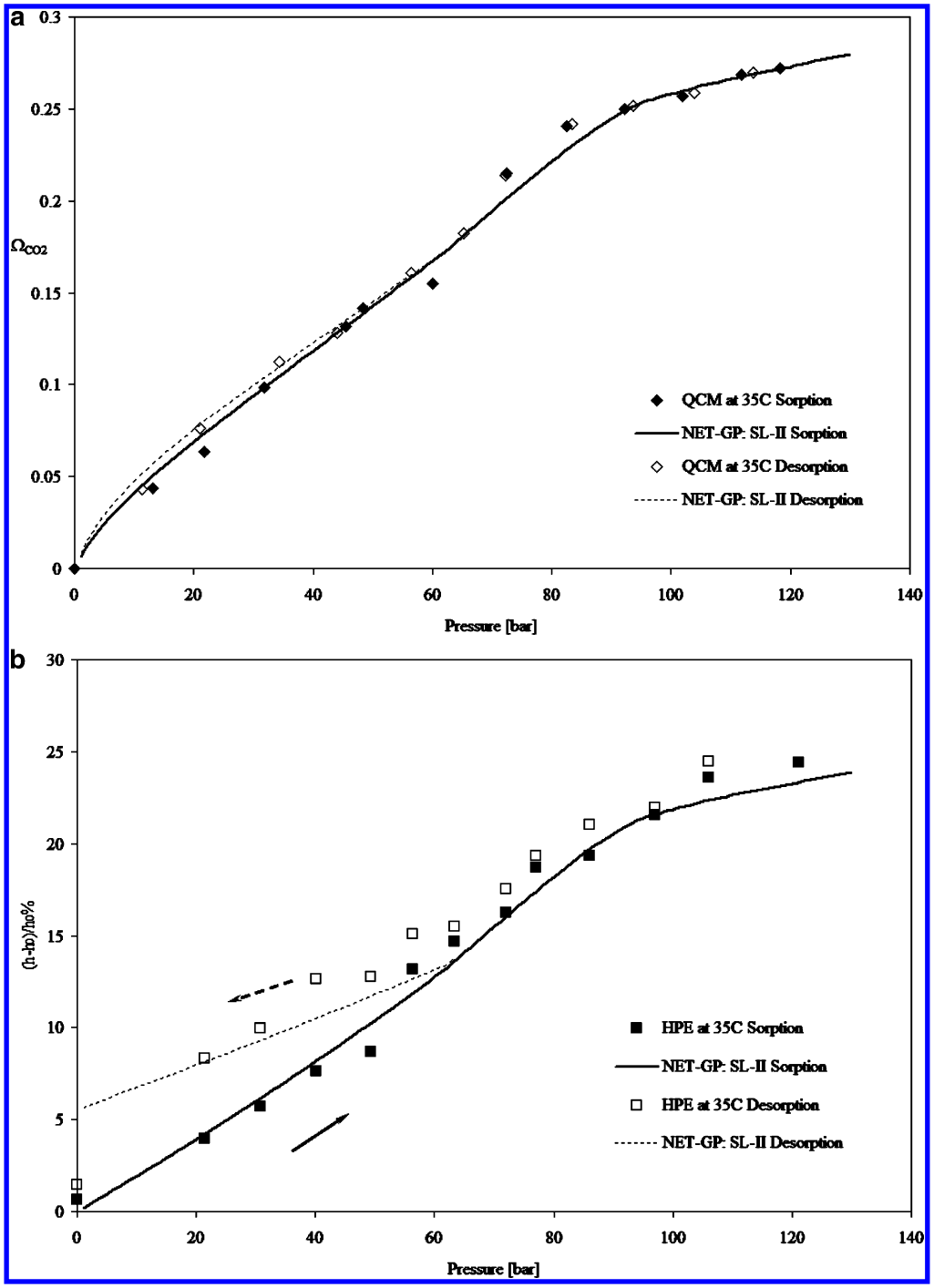

Figure 9. (a) Solubility isotherm for sorption−desorption cycle of CO_2 in PMMA at 50 °C: comparison between experimental data and fitted results using the NET-GP SL-II theory. (b) Volume swelling isotherm for sorption of CO_2 in PMMA at 35 °C: comparison between experimental data and predicted results from NET-GP SL-II theory.

Table 4. Comparison of Experimental[64] and Calculated Swelling Coefficients for Several Polymer−Gas Pairs at 35 °C[a]

	k_s [MPa^{-1}]		
system	exptl	calcd	error [%]
PMMA−CO_2	1.85×10^{-2}	1.80×10^{-2}	2.78
PC−CO_2	1.14×10^{-2}	1.18×10^{-2}	3.51
PC−C_2H_4	1.20×10^{-2}	1.21×10^{-2}	1.67
PS−CO_2	1.21×10^{-2}	1.23×10^{-2}	1.65

[a] The data needed for the calculations have been taken from the literature.[64,65]

Figure 8a shows QCM sorption data measured at 50 °C during both sorption and desorption cycles as the pressure is increased to 135 bar and then decreased to the atmospheric pressure. The results are compared to the predicted gas solubility calculated using NET-GP SL-II. Even though the hysteresis in CO_2 solubility for sorption−desorption cycles in this system is not very large, the model is able to represent it through the use of a different swelling coefficient (k'_S) for the desorption leg. The extra information needed for calculating the desorption curve in the glassy region has been retrieved here through the use of a fitting procedure for the swelling coefficient.

The corresponding HPE swelling data during the sorption and desorption cycle at 50 °C are shown in

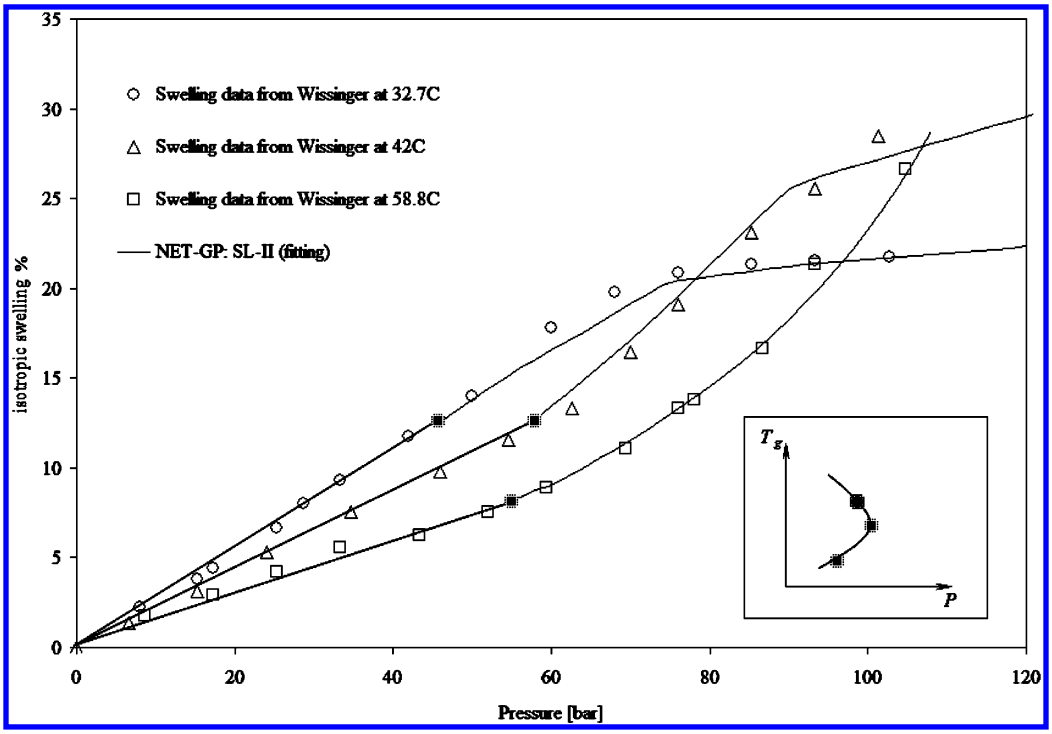

Figure 10. Volume swelling isotherm for sorption of CO_2 in PMMA at 32.7, 42, and 58.8 °C: comparison between experimental data[61] and fitting results using the NET-GP SL-II theory [thin solid lines].

Figure 8b. For comparison, Figure 8b also shows the % swelling predictions using the NET-GP SL-II. The hysteresis in the measured system volume between sorption and desorption below P_g^{50} is clearly evident in the experimental data. The model is able to obtain a fairly accurate quantitative comparison on the magnitude of the % swelling hysteresis, at least close to the glass transition, but it is not able to predict very well the values at lower pressure.

This large disparity between the model and the experimental data at low pressures is probably due to the assumption of linearity of polymer density with pressure in desorption as well as sorption. Whereas this assumption, based on experimental evidence, has been useful for modeling sorption, apparently it does not hold true in desorption for the entire pressure range. It seems to be a reasonable approximation near the glass transition point, but it does not carry forward as the pressure goes to atmospheric. This assumption is also responsible for the predicted nonzero value of the swelling at zero pressure.

Figure 9a shows the measured solubility of carbon dioxide by QCM in terms of grams of CO_2 absorbed per gram of polymer (Ω_{CO_2}) during a sorption−desorption cycle at 35 °C, a temperature just above the critical temperature for CO_2. Also shown are the comparisons to calculated values using the NET-GP SL-II model with parameters fit with solubility data during the sorption step above 100 bar at 35 °C. The binary interaction parameters for both the SL-I and SL-II models at this temperature are also shown in Table 3. Chow's theory in eq 16 predicts that the CO_2 mass density at the glass transition point corresponds to a value of $\Omega_{CO_2} = 0.171$. Using the NET-GP SL II model, the value of the glass transition pressure at 35 °C was estimated to be $P_g^{35} =$ 62 bar, very close to the measured value. In the figure the sorption isotherm for CO_2 in PMMA at 35 °C has been predicted by means of the equilibrium SL-II equation of state above P_g^{35} and the NET-GP SL-II model below that limit. A comparison of the experimental and predicted results reveals that the model provides an accurate representation throughout the whole pressure range, as the polymer changes from glassy to rubbery and the penetrant transits from vapor to a supercritical fluid.

Table 5. Interaction Parameters for the SL-II Model[a]

binary parameters	SL-II	binary parameters	SL-II
k_{ij}^{33}	0.099	η_{ij}^{42}	−0.080
η_{ij}^{33}	0.078	k_{ij}^{59}	0.077
k_{ij}^{42}	0.091	η_{ij}^{59}	−0.161

[a] Parameters fit to data above 80 bar for each tempertaure.

Figure 9b shows the corresponding % swelling of PMMA measured by HPE during the sorption−desorption cycle at 35 °C, together with the NET-GP SL-II predictions. The linear volume dilation below the glass transition pressure is evident as well as the hysteresis in measured film thickness below P_g during sorption and desorption runs. The results from the NET-GP SL-II model provide a good representation of the complex swelling behavior of this system for sorption process in the whole pressure range and for desorption process as long as the pressure is above 20 bar, the point below which the linear density variation with pressure assumption during dilation apparently fails in reproducing the experimental results, as discussed above.

Finally, in Figure 10 a comparison is shown between the predictions of the NET-GP SL-II model and swelling data for CO_2 sorption in PMMA measured by Wissinger and Paulaitis.[30] The binary interaction parameters for this calculation were estimated by fitting the swelling data at high pressure, and the results are summarized in Table 5. The initial densities of the polymer samples used in the NET-GP SL-II calculations were not reported by Wissinger and Paulaitis,[75] but they were estimated by the procedure described in the model

development section of this work. Little squares in the figure mark the glass transition point as estimated here from Chow's theory. The highest glass transition pressure is that at 42 °C because P_g experiences a maximum with temperature. This feature, reported by Condo et al.,[33] has been called "retrograde vitrification" and can be explained by considering the Chow's theory and the sorption behavior vs pressure at different temperatures. As the temperature increases, the amount of carbon dioxide needed for the transition decreases but also the sorption isotherm decreases, as result of the two opposite effects there is a maximum of P_g vs temperature as shown in the little inbox of the figure. It is encouraging that our model coupled with Chow's equation is able to predict such a complex behavior.

5. Conclusions

This work describes an extension of the nonequilibrium thermodynamics of glassy polymer (NET-GP) model for swelling and sorption to the case of a high-pressure plasticizing penetrant. The theory of Chow is used to estimate the penetrant concentration at the glass transition point, which can then be used to estimate the pressure at the glass transition point using the equilibrium equation of state for the rubber phase. By assuming there is a linear relation between the glassy polymer density and the pressure below the glass transition pressure, it is possible to estimate the dilatation or swelling coefficient for the polymer−penetrant system. This facilitates the calculation of the sorption and swelling behavior by modeling the system using NET-GP below the glass transition pressure and the equilibrium equation of state above the glass transition pressure. The NET-GP approach can be used with any equilibrium equation of state that is capable of predicting the behavior of the system in the rubbery state. As a result, this is a very flexible approach that can be used for any equation of state regardless of its complexity. Use of the theory relies on knowledge of the initial density of the glassy polymer prior to solvent penetration. For cases, in which the initial polymer density is not known or is not provided, a procedure is described that facilitates its estimation based on the magnitude of the swelling coefficient.

The new model was applied to the interpretation of experimental data collected for sorption/desorption processes of CO_2 in PMMA films at different temperatures and for a wide range of CO_2 pressures. Swelling of PMMA was measured using high-pressure ellipsometry (HPE) and mass absorption was measured directly by use of a quartz crystal microbalance (QCM). The mass of absorbed CO_2 was also determined indirectly from the measured refractive index of the swollen film resulting from the ellipsometric analysis.

One of the major experimental findings of this work is that the sorption and swelling behaviors of two samples of a glassy polymer are the same as long as their densities are the same, even though their histories can be significantly different. To the best of our knowledge, this is the first experimental verification of the basic assumption of the NET-GP model, namely, that the glass polymer density can be used as order parameter to describe the nonequilibrium thermodynamic state of the system.

Through the use of a nonequilibrium version of the Sanchez−Lacombe lattice fluid model with two binary interaction parameters (NET-GP SL-II model), gas solubility and volume dilation were correctly represented at all experimental conditions. The model was able to provide a remarkably good agreement with the swelling hysteresis observed experimentally upon sorption and desorption of the gas, except for pressures close to atmospheric in desorption runs, where there is an apparent breakdown in the assumption of linearly of density with pressure.

The model also was able to provide an accurate description of the glass transition pressure variation with temperature as well as of the amount of gas absorbed in the glassy polymer phase. The work presented here can serve as the basis for future development in the study of the dynamic and equilibrium properties of high-pressure gas−polymer systems.

Acknowledgment. The authors thank the Kenan Center for the Utilization of Carbon Dioxide in Manufacturing at NC State University and the University of Bologna for their funding of this work. This work was also supported in part by the Italinan Ministry (MIRST) and the STC Program of the National Science Foundation under Agreement CHE-9876674.

Notation

a = Helmholtz free energy density (kcal kg^{-1})
C_m = QCM mass coefficient
C_p = QCM pressure coefficient
ΔC_P = constant pressure specific heat (J kg^{-1} K^{-1})
f = fugacity
F, F_0 = QCM frequencies (MHz)
ΔF_m = mass contribution to the frequency (MHz)
ΔF_P = pressure contribution to the frequency (MHz)
ΔF_η = viscosity contribution to the frequency (MHz)
h, h_0 = sample thickness (μm)
k_{ij} = binary energetic interaction parameter
k_S = swelling coefficient (MPa^{-1})
Δm = adsorbed mass (μg cm^{-2})
M_{wj} = molecular weight (kg kmol^{-1})
n_j = number of moles (mol)
$\langle n_j \rangle$ = refractive index
$\langle n_f \rangle$ = mixture refractive index
P = pressure (bar)
q = HPE coefficient (cm^3 g^{-1})
r = number of mers
R = gas constant (J mol^{-1} K^{-1})
R_j = molar refraction
T = temperature (K)
v^* = Sanchez−Lacombe volumetric parameter (cm^3)
z = coordination number
Z = compressibility
ϵ^* = Sanchez−Lacombe energetic parameter (J mol^{-1})
ϕ = volume fraction
φ = fugacity coefficient
η_q, η_f = shear viscosities (kg m^{-1} s^{-1})
η_{ij} = binary volumetric interaction parameter
μ_j = chemical potential (J mol^{-1})
θ = Chow's theory parameter
ρ_j, ρ_q, ρ_f = densities (g cm^{-3})
Σ = state
ω = mass fraction
Ω = mass ratio
Ψ = Chow's theory parameter

Subscripts

i, j = generic component in the mixture
1, CO_2 = carbon dioxide
2, PMMA = polymer
mix = mixture
m = mass
P = pressare
q = quartz

f = fluid
p = polymer
d = diluent
g = glassy/rubbery transition
Superscripts
0 = referring to the initial conditions
(s) = solid phase
NE = nonequilibrium
eq = equilibrium
∞ = asymptotic value
g = glassy/rubbery transition
res = residual
35, 50 = referring to a particular temperature
mix = mixture

References and Notes

(1) McHugh, M. A.; Krukonis, V. J. *Supercritical Fluid Extraction: Principles and Practice;* Butterworth: Boston, 1986.
(2) McHugh, M. A.; Krukonis, V. J. *Encyclopedia of Polymer Science and Technology;* Mark, H. F., Bikales, N. M., Overberger, C. G., Menges, G., Eds.; Wiley-Interscience: New York, 1989; Vol. 16, p 368.
(3) Daneshvar, M.; Gulari, E. In *Supercritical Fluid Science and Technology;* Johnston K. P., Penninger, J. M. L., Eds.; ACS Symposium Series 406; American Chemical Society: Washington, DC, 1989.
(4) Canelas, D. A.; Betts, D. E.; DeSimone, J. M.; Yates, M. Z.; Johnston, K. P. *Macromolecules* **1998**, *31*, 6794.
(5) Yates, M. Z.; Li, G.; Shim, J.-J.; Johnston, K. P.; Lim, K. T.; Webber, S. *Macromolecules* **1999**, *32*, 1018.
(6) Kiran, E.; Saraf, V. P.; Sen, Y. L. *Int. J. Thermophys.* **1989**, *10*, 437.
(7) Wang, W.-C. V.; Kramer, E. J.; Sachse, W. H. *J. Polym. Sci., Polym. Phys. Ed.* **1982**, *20*, 1371.
(8) Chiou, J. S.; Barlow, J. W.; Paul, D. R. *J. Appl. Polym. Sci.* **1985**, *30*, 2633.
(9) Hachisuka, H.; Sato, T.; Imai, T.; Tsujita, Y.; Takizawa, A.; Kinoshita, T. *Polym. J.* **1990**, *22*, 77.
(10) Wissinger, R. G.; Paulatis, M. E. *J. Polym. Sci., Part B: Polym. Phys.* **1991**, *29*, 879.
(11) Hoy, K. L.; Donhue, M. D. *Polym. Prepr.* **1990**, *31*, 679.
(12) Cooper, A. I. *Mater. Chem.* **2000**, *10*, 207.
(13) Novick, B. J.; Carbonell, R. G.; DeSimone, J. M. *Proceedings of the 5th International Symposium of Supercritical Fluids*, April 2000.
(14) DeSimone, J. M.; Guan, Z.; Eisbernd, C. S. *Science* **1992**, *257*, 945.
(15) Flores, P. A. PCT Int. Appl. 2004.
(16) Kazarian, S. G. *Drugs Pharm. Sci.* **2004**, *138*, 343.
(17) Dixon, D. J.; Johnston, K. P.; Bodmeier, M. A. *AIChE J.* **1993**, *39*, 127.
(18) Watkins, J. J.; Blackburn, J. M.; McCarthy, T. J. *Chem. Mater.* **1999**, *11*, 213.
(19) Howdle, S. M.; George, M. W.; Poliakoff, M. In *Chemical Synthesis Using Supercritical Fluids*; Jessop, P. G., Leiner, W., Eds.; Wiley-VCH: Weinheim, 1999.
(20) Weibel, G. L.; Ober C. K *Microelectron. Eng.* **2003**, *65*, 145.
(21) Pope, D. S.; Koros, W. J. *Macromolecules* **1992**, *25*, 1711.
(22) Shim, J.-J.; Johnston, K. P. *AIChE J.* **1989**, *35*, 1097.
(23) Shim, J.-J.; Johnston, K. P. *J. Phys. Chem.* **1991**, *95*, 353.
(24) Shim, J.-J.; Johnston, K. P. *AIChE J.* **1991**, *37*, 607.
(25) Sand, M. L. Method for Impregnating a Thermoplastic Polymer, US Patent #4,598,006, 1986.
(26) Kazarian, S. G.; Vincent, M. F.; West, B. L.; Eckert, C. A. *J. Supercrit. Fluids* **1998**, *13*, 107.
(27) Gallacher-Wetmore, P.; Ober, C. K.; Gabor, A. H.; Allen, R. D. *Proc. SPIE—Int. Soc. Opt. Eng.* **1996**, *289*, 2725.
(28) Gabor, A. H.; Allen, R. D.; Gallacher-Wetmore, P.; Ober, C. K. *Proc. SPIE—Int. Soc. Opt. Eng.* **1996**, *410*, 2724.
(29) Sundararajan, N.; Yang, S.; Ogino, K.; Valiyaveettil, S.; Wang, J.; Zhou, X.; Ober, C. K.; Obendorf, S. K.; Allen, R. D. *Chem. Mater.* **2000**, *12*, 41.
(30) Wissinger, R. G.; Paulatis, M. E. *Ind. Eng. Chem. Res.* **1991**, *30*, 842.
(31) Barbari, T. A.; Conforti, R. M. *Polym. Adv. Technol.* **1994**, *5*, 698.
(32) Zhang, Y.; Gangwani, K. K.; Lemert, R. M. *J. Supercrit. Fluids* **1997**, *11*, 115.
(33) Condo, P. D.; Sanchez, I. C.; Panayiotou, C. G.; Johnston, K. P. *Macromolecules* **1992**, *25*, 6119.
(34) Doghieri, F.; Ghedini, M.; Quinzi, M.; Rethwisch, D. G.; Sarti, G. C. In *Advanced Materials for Membrane*; Pinnau, I., Freeman, B. D., Eds.; *ACS Symp. Ser.* **2004**, *876*, 55−73.
(35) Doghieri, F.; Sarti, G. C. *Macromolecules* **1996**, *29*, 7885.
(36) Sarti, G. C.; Doghieri, *F. Chem. Eng. Sci.* **1998**, *53*, 3435.
(37) Doghieri, F.; Sarti, G. C. *J. Membr. Sci.* **1998**, *147*, 73.
(38) Chow, T. S. *Macromolecules* **1980**, *13*, 362.
(39) Wind, J. D.; Sirard, S. M.; Paul, D. R.; Green, P. F.; Johnston, K. P.; Koros, W. J. *Macromolecules* **2003**, *36*, 6433.
(40) Sirard, S. M.; Green, P. F.; Johnston, K. P. *J. Phys. Chem. B* **2001**, *105*, 766.
(41) Scmidt, J. W.; Moldover, M. R. *J. Chem. Phys.* **1993**, *99*, 582−589.
(42) Johs, B. *Accurate Correction of Window Effects in Ellipsometric Data;* J.A. Woollam Co., Inc., 9/7/99.
(43) Johs, B. *Methods for uncorrelated evaluation of parameters in parametrized mathematical equations for window retardance, in ellipsometer and polarimeter systems,* US Patent #6,034,777.
(44) Herzinger, C. M.; Johs, B.; McGahan, W. A.; Woollam, J. A.; Paulson, W. *J. Appl. Phys.* **1998**, *83*, 3323.
(45) Michels, A.; Hamers, J. *Physica IV* **1937**, 995.
(46) Obriot, J.; Ge, J.; Bose, T. K.; St-Arnaud, J. M. *Fluid Phase Equilib.* **1993**, *86*, 315.
(47) Tompkins, H. G.; McGahan, W. A. *Spectroscopic Ellipsometry and Reflectometry*; John Wiley & Sons: New York, 1999.
(48) Stamatialis, D. F.; Wessling, M.; Sanopoulou, M.; Strathmann, H.; Petropoulos, J. H. *J. Membr. Sci.* **1997**, *130*, 75.
(49) Bolton, B. A.; Kint, S.; Bailey, G. F.; Scherer, J. R. *J. Phys. Chem.* **1986**, *90*, 1207.
(50) Fleming, G. K.; Koros, W. J. *J. Polym. Sci., Part B: Polym. Phys.* **1987**, *25*, 2033.
(51) Orwoll, R. A. In *Physical Properties of Polymers Handbook*; Mark, J. E., Ed.; American Institute of Physics: Woodbury, NY, 1996.
(52) Wu, Y. T.; Akoto-Ampaw, P. J.; Elbaccouch, M.; Hurrey, M. L.; Wallen, S. L.; Grant, C. S. *Langmuir* **2004**, *20*, 3665.
(53) Miura, K.-I.; Otakeb, K.; Kurosawab, S.; Sakob, T.; Sugetab, T.; Nakaneb, T.; Satob, M.; Tsujia, T.; Hiakia, T.; Hongoa, M. *Fluid Phase Equilib.* **1998**, *144*, 181.
(54) Sauerbrey, G. *Z. Phys.* **1959**, *155*, 206.
(55) Lu, C. S.; Lewis, O. *J. Appl. Phys.* **1972**, *43*, 4385.
(56) Kanazawa, K. *Faraday Discuss.* **1997**, *107*, 77.
(57) White, C. C.; Schrag, J. L. *J. Chem. Phys.* **1999**, *111*, 24, 11192.
(58) Lucklum, R.; Hauptmann, P. *Electrochim. Acta* **2000**, *45*, 3907.
(59) Stockbridge, C. D., Behrndt, K. H., Eds.; In *Vacuum Microbalance Techniques*; Plenum: New York, 1966; Vol. 5, pp 147−191.
(60) Kanazawa, K. K.; Gordon, J. G., II *Anal. Chem. Acta* **1985**, *175*, 99.
(61) Astarita, G.; Paulatis, M. E.; Wissinger, R. G. *J. Polym. Sci., Part B: Polym. Phys.* **1989**, *27*, 2105.
(62) Roe, R.-J. *J. Appl. Phys.* **1977**, *48*, 4085.
(63) Doghieri. F.; Ghedini, M.; Quinzi, M.; Rethwisch, D.; Sarti, G. C. *Desalination* **2002**, *144*, 73.
(64) Giacinti Baschetti, M.; Doghieri, F.; Sarti, G. C. *Ind. Eng. Chem. Res.* **2001**, *40*, 3027.
(65) Varma-Nair, M.; Wunderbelich, B. *J. Phys. Chem. Ref. Data* **1982**, *11,* 1985.
(66) Royer, J. R.; DeSimone, J. M.; Khan, S. A. *J. Polym. Sci., Part B: Polym. Phys.* **2001**, *39*, 3055.
(67) Condo, P. D.; Paul, D. R.; Johnston, K. P. *Macromolecules* **1994**, *27*, 365−371.
(68) Wissinger, R. G.; Paulatis, M. E. *J. Polym. Sci., Part B: Polym. Phys.* **1987**, *25*, 2497.
(69) Sanchez, I. C.; Lacombe, R. H. *J. Phys. Chem.* **1976**, *80*, 2352.
(70) Lacombe, R. H.; Sanchez, I. C. *J. Phys. Chem.* **1976**, *80*, 2568.
(71) Sanchez, I. C.; Lacombe, R. H. *Macromolecules* **1978**, *11*, 1145.
(72) Neau, E. *Fluid Phase Equilib.* **2002**, *203*, 133.
(73) Kirby, C. F.; McHugh, M. A. *Chem. Rev.* **1999**, *99*, 565.
(74) Pham, J. Q.; Sirard, S. M.; Johnston, K. P.; Green, P. F. *Phys. Rev. Lett.* **2003**, *91*, 17.
(75) Wissinger, R. G.; Paulatis, M. E. *J. Polym. Sci., Part B: Polym. Phys.* **1987**, *25*, 2497.

MA0506684